



DOI: doi.org/10.21009/SPEKTRA.073.04

THE DENSITY FUNCTIONAL THEORY STUDY OF Li-ION DIFFUSION IN Na-DOPED $\text{Li}_4\text{Ti}_5\text{O}_{12}$ AS LITHIUM-ION BATTERY ANODE

Achda Fitriah¹, Anugrah Azhar², Adam Badra Cahaya¹, Edi Suprayoga³,
Muhammad Aziz Majidi^{1,*}

¹Department of Physics, Faculty of Mathematics and Natural Sciences, University of Indonesia, Depok 16424, Indonesia

²Physics Study Program, Faculty of Sciences and Technology, Syarif Hidayatullah State Islamic University Jakarta, South Tangerang 15412, Indonesia

³Research Center for Quantum Physics, National Research and Innovation Agency (BRIN), South Tangerang 15214, Indonesia

*Corresponding Author Email: aziz.majidi@sci.ui.ac.id

Received: 30 September 2022
Revised: 11 November 2022
Accepted: 13 November 2022
Online: 30 November 2022
Published: 30 December 2022

SPEKTRA: Jurnal Fisika dan Aplikasinya
p-ISSN: 2541-3384
e-ISSN: 2541-3392



ABSTRACT

Spinel phase lithium titanate ($\text{Li}_4\text{Ti}_5\text{O}_{12}$ or LTO) has been studied as an alternative anode material with a “zero-strain” characteristic structure to improve safety, cycling stability, and rate performance. LTO offers stable Li-ion diffusion at a higher charge-discharge rate without noticeable structural change. However, LTO exhibits low electronic conductivity and low Li-ion diffusion compared to graphite-based anode materials, limiting its rate capability. In this study, we investigate the impact of Na atom doping on the diffusion rate in the $\text{Li}_4\text{Ti}_5\text{O}_{12}$ (LTO) spinel phase using the density functional theory (DFT). Based on the nudged elastic band (NEB) calculation, we obtain the energy barrier values and each diffusion pathway, with barrier energy varying about 0.3~0.4 eV and affecting the value of the diffusion constant obtained. The study reveals the role of Na atom doping in the lithium-ion diffusion in $\text{Na}_x\text{Li}_{4-x}\text{Ti}_5\text{O}_{12}$ for battery anode material.

Keywords: lithium-ion battery, lithium titanate, Li-ion diffusion, DFT

INTRODUCTION

The study of the development of lithium-ion batteries (LIBs) is becoming more advanced due to the increasing demand for energy storage devices with large specific energy densities for the needs of small mobile electronic devices such as mobile phones and laptops to large ones such as electric vehicles. Electric vehicles have now become an alternative that has attracted much attention because of their low impact on the environment compared to conventional vehicles with internal combustion engines [1]. Much effort has been directed to studying LIBs development in the automotive industry. However, some problems are often found in terms of safety, speed charging, and decrease of performance decreases during use [2]. The electrode's working mechanism influences battery life during operation with the main working principle of intercalation and deintercalation. To understand this process, it is necessary to study the dynamics of Li ions which are governed by the activation energy of ion jumps between interstitial or vacancy sites. Due to the importance of Li diffusion in LIBs, Li diffusion properties are often investigated, such as barrier energy and diffusion pathways [3-6].

The impact of this diffusion process usually causes the formation of cracks that can damage the cell due to changes in the electrode volume. Therefore, electrodes that can withstand the distortion of the structure are needed. One of the potential materials as anodes for LIBs for future generations is titanate-based materials such as lithium titanate $\text{Li}_4\text{Ti}_5\text{O}_{12}$ (LTO) spinel phase which has good stability and safety. Many attempts have been made to improve the performance of LTO through various metal doping, one of which is Na doping [7]. This Na doping is expected to increase the Li diffusivity in the LTO spinel structure.

Recently, there was a report on the doping of Na atoms to the spinel phase LTO crystals which were confirmed to have a basic crystal structure identical to that of the spinel phase LTO and suitable to be used as a potential anode material candidate [4]. The experimental results also revealed that Na doping in the spinel phase LTO will increase the lattice parameters so that the crystal volume also increases, correlated with the lithium-ion diffusivity [7]. However, the Li diffusion mechanism has not been discussed in detail elsewhere, such as barrier energy, Li-ion diffusion pathways, and diffusivity coefficient at the Na-doped LTO structure. Therefore, in this study, we focus on the diffusion capability of Li vacancy at the LTO anode with the formula $\text{Na}_x\text{Li}_{4-x}\text{Ti}_5\text{O}_{12}$, where x is the amount of Na-doped. The values of $x = 0, 0.5, 1$ were chosen as they correspond to manageable supercell size in the simulation. To explain the Li diffusion mechanism, we investigate the change in barrier energy and its comparison to the anode pure spinel phase LTO.

In particular, the details of the Li diffusion mechanism in the spinel phase LTO with Na doping is carried out theoretically using the first-principle calculation through a quantum mechanical approach known as Density Functional Theory (DFT). The DFT calculation effectively investigates atomic diffusion based on the Nudged Elastic Band (NEB) method [8] and allows us to simulate the Li diffusion pathway.

METHOD

Supercell Structural Model of $\text{Na}_x\text{Li}_{4-x}\text{Ti}_5\text{O}_{12}$

The LTO structure used for the calculation is the spinel phase LTO with the chemical formula $\text{Li}_4\text{Ti}_5\text{O}_{12}$. The supercell structure was built from previous work with the composition $\text{Li}_6^{8a}(\text{Li}_2\text{Ti}_{10})^{16d}\text{O}_{24}^{32e}$ space group C2/c [9]. 75% of the Li atoms occupy the 8a site with a tetrahedral symmetry group, and the rest are at the 16d site with an octahedral symmetry group [10] as shown in FIGURE 1. a). The spinel phase LTO supercell then be made an LTO model with Na doping to different Li sites, namely 16d and 8a sites with the amount of Na-doped is $x = 0, 0.5, 1$, so that the composition becomes $(\text{NaLi}_5)^{8a}(\text{Li}_2\text{Ti}_{10})^{16d}\text{O}_{24}^{32e}$, $(\text{Li}_6)^{8a}(\text{NaLiTi}_{10})^{16d}\text{O}_{24}^{32e}$, and $(\text{NaLi}_5)^{8a}(\text{NaLiTi}_{10})^{16d}\text{O}_{24}^{32e}$ as shown in FIGURE 1. b).

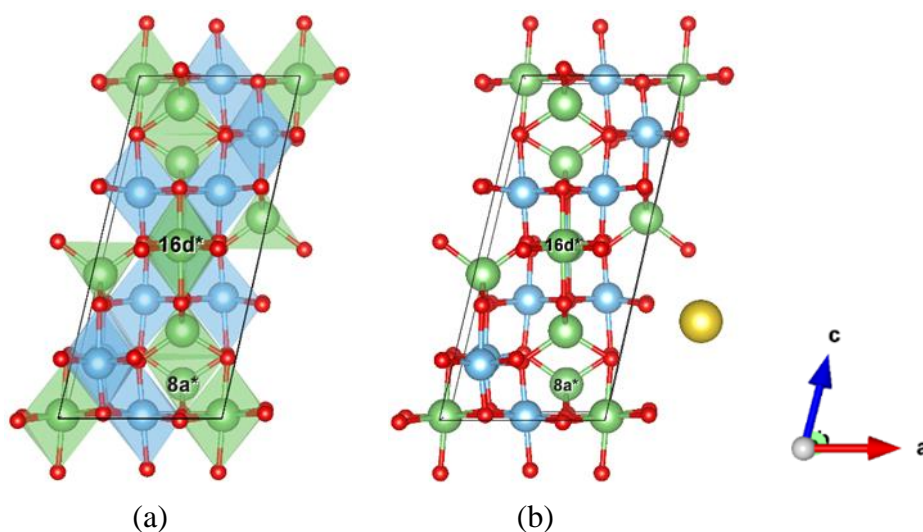


FIGURE 1. Structure of a) pure and b) Na-doped spinel LTO supercell at sites 16d and 8a. The dotted line indicates the Li atom is at the 16d site. The 16d* and 8a* sites are the Na atom doping sites. The green, blue, yellow, and red spheres are lithium ions, respectively (sites 8a, 16d); titanium (16d); sodium (16d, 8a); and oxygen (32e). The tripod indicates the direction of the supercell structure. (Images were generated using the VESTA software package) [11].

Lithium Vacancy Diffusion

Furthermore, the vacancy site under consideration is a tetrahedral type 8a site where one Li atom is surrounded by four O atoms in the spinel phase LTO material. The respective vacancies marked with the letters A and B are shown in FIGURE 2. The diffusion pathway was chosen based on previous work [3] because it has a perfectly symmetrical shape of the path through which Li ions are most likely to pass. Therefore, the other paths are ignored because the selected diffusion path will represent the other paths. To investigate the Li diffusion mechanism by vacancy jump, only one Li vacancy per supercell would be required. After that, the structure optimization was carried out for each vacancy by maintaining the cell parameters, and only the atomic position could be changed.

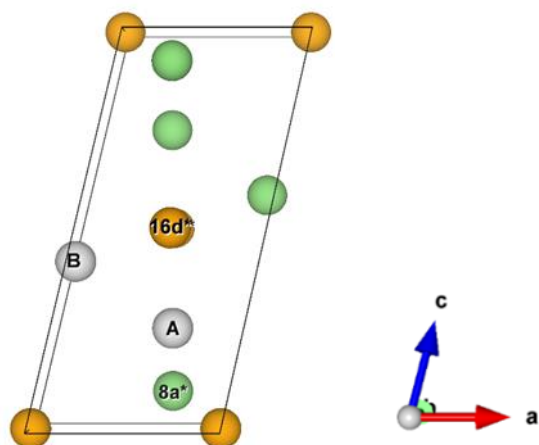


FIGURE 2. The structure of the Li vacancy and the vacancy diffusion pathway at site 8a of A→B. The lithium ion sites 8a and 16d are colored in green and orange, while the vacancy sites are colored in gray. The 16d* and 8a* sites are the Na atom doping sites. The path is indicated by a purple arrow. The tripod indicates the direction of the supercell structure. (Image generated using the VESTA software package) [11].

In this work, the selected diffusion pathway connects two types of tetrahedral sites. To identify the diffusion pathway, we will then calculate the activation barrier energy ΔE associated with defect jump rates Γ using the Arrhenius equation [5].

$$\Gamma = \nu e^{-\Delta E/k_B T} \quad (1)$$

where ν is the frequency factor, T is the absolute temperature, and k_B is the Boltzman constant. From EQUATION (1), we will get the diffusion constant of the vacancy diffusion path with the following equation.

$$D = l^2 \Gamma \quad (2)$$

where D is the diffusion constant, and l is the atomic jump distance.

Computational Methods

All DFT calculations in this work were carried out using the PWscf code [12] Quantum Espresso with a plane wave basis to express the wave function on the valence electrons. The Pseudopotential Perdew-Burke-Emzerhof (PBE) is used to represent the electron nucleus and atomic nucleus [13]. Then, general gradient approximations (GGA) were used on PBE parameterization for the exchange-correlation function. Several other parameters used are energy cut-off wave function and electron density of ~ 90 and ~ 900 Ry. The number of k-points taken is $4 \times 4 \times 1$ using Monkhorst-Pack (MP) [14]. Furthermore, the atomic position and cell size are fully relaxed for structural optimization until the force acting on the remaining atoms is less than 10^{-6} eV/Å. Minimum energy paths (MEP) in this diffusion phenomenon is carried out using the Nudged Elastic Band (NEB) calculation method to obtain the energy barrier of the diffusion path under review [15]. The MEP is estimated by fitting the spline polynomial to the energy and energy gradient of the image. In this calculation, the particle trajectory is created by linear interpolation between the initial and final images with a climbing image parameter applied to a total of five images to ensure the correct location of the activation

barrier. The threshold for the total force, which is acting on the reaction pathway considered to be convergent when the acting force is lower than 0.05 eV/\AA .

RESULT AND DISCUSSION

Optimized supercell and vacancies structure of $\text{Na}_x\text{Li}_{4-x}\text{Ti}_5\text{O}_{12}$

The supercell structure resulting from our DFT calculations has the most stable condition with the lattice parameters summarized in Table 1, which results in an expansion of the volume in the LTO with Na doping of about 2 to 4%. The volume change here is due to the spatial adjustment due to Na doping towards the Li atom, which has a larger ionic mass and radius. This is the following experiment [7] that doping a number of Na atoms can increase the cell size so that the lattice parameter increases.

TABLE 1. Optimized result geometry data of $\text{Na}_x\text{Li}_{4-x}\text{Ti}_5\text{O}_{12}$ structure in 16d and 8a sites. (a , b , and c are lattice constant and V is the volume of LTO structure.)

Parameters	Mount of Na doping in LTO spinel phase			
	Column Header			
	$x = 0$	$x = 0.5$ (16d)	$x = 0.5$ (8a)	$x = 1$ (16d, 8a)
a [\AA]	5.821	5.826	5.850	5.852
b [\AA]	5.821	5.884	5.844	5.908
c [\AA]	12.956	13.146	13.118	13.317
V [\AA^3]	417.986	427.090	426.515	436.069

The data in TABLE 1. shows the effect of Na doping on the structure of $\text{Na}_x\text{Li}_{4-x}\text{Ti}_5\text{O}_{12}$ which shows an increase in lattice parameters and cell volume due to doping of a number of Na atom. When $\text{Na}_{x=0.5}$ was doped, we selected two different sites to determine the effect of Na doping on sites 8a and 16d where both sites were close to the lithium vacancy site to maximize the repulsion between atoms so that the area around the vacancy becomes more tenuous. Doping $\text{Na}_{x=0.5}$ at sites 16d and 8a significantly enlarged all of lattice parameters than the LTO pure. This proves that the substitution of Na at certain sites can affect the lattice structure parameters bigger. However, when observed from the change in volume, $\text{Na}_{x=0.5}$ doping at site 16d resulted in an increase in volume similar to site 8a which concluded that Na doping at different sites did not affect the volume change. Furthermore, $\text{Na}_{x=1}$ doping at both sites resulted in an increase in all of lattice parameters than the LTO pure and $\text{Na}_{x=0.5}$ doping so that the volume increased by 2% of the structure with $\text{Na}_{x=0.5}$ doping. Increasing a number of lattice parameters and also cell volume is an important factor that can affect the diffusivity of the vacancy. Doping the Na atom adds electrons to the LTO structure so that the number of electrons increases and its density increases. It can theoretically expand the lattice parameters and lower the energy barrier to help the Li-ions diffuse. However, to prove it, further investigation is needed on the energy barrier of the vacancy diffusion pathway which will be discussed in the next section.

Lithium Vacancy Diffusion

The NEB calculation to calculate the barrier energy and the transition state of the pure spinel and Na-doped LTO connecting the two Li vacancy sites reaches the convergence as shown in FIGURE 3. a). The perfectly symmetrical shape of the diffusion path is generated by reference to the previous work by Benedict et al [3]. Only one resulting path does not stabilize the transition state (meta), namely when doping $\text{Na}_{x=1}$. This NEB pathway explains the Li vacancy's movement, while the Li-ion position displacement can be seen in FIGURE 3.b).

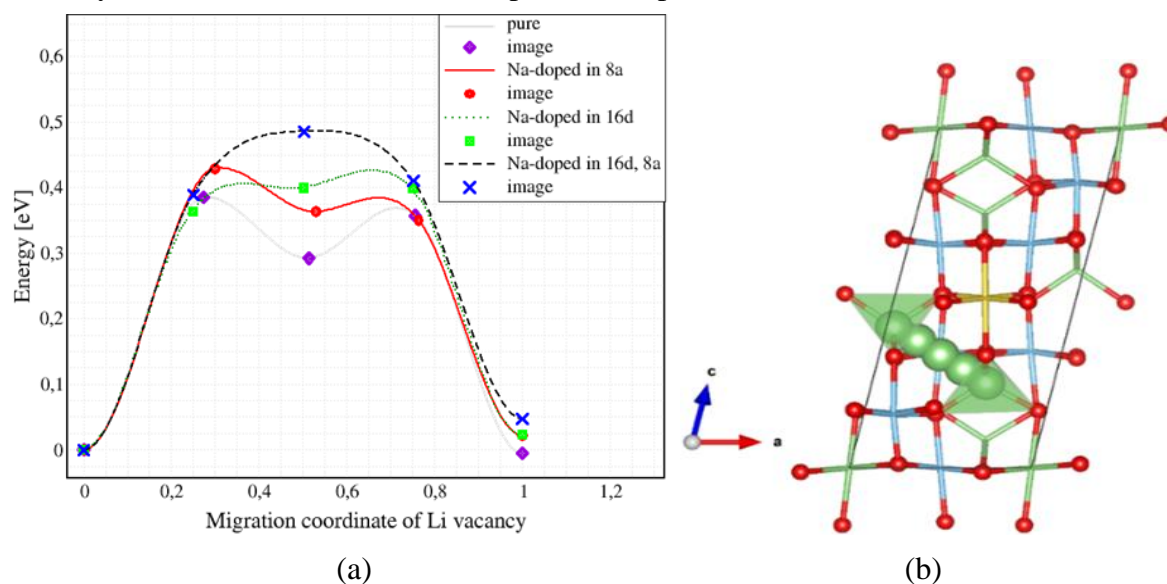


FIGURE 3. Investigation of a) activation barrier and b) diffusion of Li ions in pure spinel and Na-doped LTO. The green ball represents the movement of Li ions while the red ball represents oxygen. (Figure (b) generated with the VESTA software package) [9].

It can be seen in FIGURE 3. b) the image of the movement of Li ions in the $\mathbf{A} \rightarrow \mathbf{B}$ vacancy explains why the energy curve looks symmetrical, which means that this diffusion path is possible for Li-ions to pass. For ion transport along the diffusion pathway, the Li vacancy occurs with a jump length of about 3.6 \AA . For information, the jump length corresponds to the lattice constant. If the lattice constant is large, the jump length will increase. Further, the energy barrier should not be too high because it will make Li-ions difficult to move, or too low as it will make Li-ions unable to find possible stopping positions. The obtained diffusion path barrier energy was used to calculate the diffusivity, summarized along with the jump length and barrier energy in TABLE 2. The diffusivity standard varies according to the results of previous studies from $10^{-11} \sim 10^{-17} \text{ cm}^2 \cdot \text{s}^{-1}$ [16].

TABLE 2. Jump length, activation barrier, and diffusivity for Li transport in $\text{Na}_x\text{Li}_{4-x}\text{Ti}_5\text{O}_{12}$ structure.

Mount of Na doping in LTO	Jump length l [\AA]	Activation barrier, ΔE^{\rightarrow} [eV]	Activation barrier, ΔE^{\leftarrow} [eV]	DFT calculated diffusivity, D^{\rightarrow} [$\text{cm}^2 \cdot \text{s}^{-1}$]	DFT calculated diffusivity, D^{\leftarrow} [$\text{cm}^2 \cdot \text{s}^{-1}$]
$x = 0$	3.612	0.393	0.365	4.43×10^{-13}	3.38×10^{-13}
$x = 0.5$ (16d)	3.667	0.399	0.376	2.44×10^{-13}	5.94×10^{-13}
$x = 0.5$ (8a)	3.614	0.428	0.406	8.40×10^{-14}	1.97×10^{-13}
$x = 1$ (16d, 8a)	3.682	0.486	0.438	8.52×10^{-15}	5.47×10^{-14}

Channel diffusivity is calculated by EQUATION (2) with frequency factor value $\nu=10^{13} \text{ s}^{-1}$ [8]. From the graph in FIGURE 3. a), it is known that the energy curve of the diffusion path between $\text{Na}_{x=1}$ and pure doping is symmetrical with the vacancy jump barrier energy $\mathbf{A} \rightarrow \mathbf{B}$ is 0.49 eV and 0.39 eV, each of which is the highest and lowest energy. However, the energy barrier for the reverse path is lower. Next is the diffusion path doped with $\text{Na}_{x=0.5}$ at sites 16d and 8a. As seen in the curves, both show asymmetrical MEPs for forwarding and backward jumps. Calculation of the energy barrier for vacancy jumps $\mathbf{A} \rightarrow \mathbf{B}$ for $\text{Na}_{x=0.5}$ (16d), and $\text{Na}_{x=0.5}$ (8a) is 0.40 eV and 0.43 eV, while the reverse direction is lower for both. A previous study by Benedikt et al. found a Li vacancy barrier of 0.49 eV at the 8a intersite jump [3] in the pure hexagonal spinel phase $\text{Li}_4\text{Ti}_5\text{O}_{12}$, whereas, in our structure, it was 0.1 eV lower. Apart from these differences, the results in table three reveal that the increase in jump length is caused by an increase in the volume of the structure due to the doping of a number of Na atoms, where this jumping distance is strongly correlated with the diffusivity of the lithium-ion vacancy. After the calculations, we observed that the energy barrier increased when Na was doped, which did not show a positive correlation with the Li-ion diffusivity.

CONCLUSION

In this work, the diffusion properties of $\text{Na}_x\text{Li}_{4-x}\text{Ti}_5\text{O}_{12}$ were investigated using DFT. Following the experimental results, structural optimization analysis showed increased lattice and volume parameters in Na-doped LTO crystals by 2-4%. We have calculated energy barriers for the diffusion vacancy lithium that lead to various diffusivities. Our result can be compared with the experimental studies with Na and Br doping [7]. In addition, our results show an increase in the energy barrier of the Na-doped spinel-phase LTO structure, which can reduce the mobility of lithium ions during diffusion. This problem may be solved by changing the metal doping or the doping position in this spinel phase LTO structure.

ACKNOWLEDGMENTS

The computation in this work has been done using the facilities of MAHAMERU BRIN HPC, National Research and Innovation Agency of Indonesia (BRIN).

REFERENCES

- [1] M. A. Hannan *et al.*, "A review of lithium-ion battery state of charge estimation and management system in electric vehicle applications: Challenges and recommendations," *Renewable and Sustainable Energy Reviews*, vol. 78, 2017, doi: 10.1016/j.rser.2017.05.001.
- [2] A. Tomaszewska *et al.*, "Lithium-ion battery fast charging: A review," *Publisher Full Text, e-Transportation*, vol. 1, 2019, doi: 10.1016/j.etrans.2019.100011.
- [3] B. Ziebarth, *et al.*, "Lithium diffusion in the spinel phase $\text{Li}_4\text{Ti}_5\text{O}_{12}$ and in the rocksalt phase $\text{Li}_7\text{Ti}_5\text{O}_{12}$ of lithium titanate from first principles," *Phys. Rev. B - Condens. Matter Mater. Phys.*, vol. 89, no. 17, 2014, doi: 10.1103/PhysRevB.89.174301.

- [4] K. Tada, *et al.*, “A comparative study of Na₃LiTi₅O₁₂ and Li₄Ti₅O₁₂: Geometric and electronic structures obtained by density functional theory calculations,” *Chemical Physics Letters*, vol. 731, 2019, doi: 10.1016/j.cplett.2019.136598.
- [5] A. Van der Ven and G. Ceder, “Lithium diffusion mechanisms in layered intercalation compounds,” in *Journal of Power Sources*, vol. 97-98, 2001, doi: 10.1016/S0378-7753(01)00638-3.
- [6] M. Wilkening *et al.*, “Microscopic Li self-diffusion parameters in the lithiated anode material Li_{4+x}Ti₅O₁₂ (0 ≤ x ≤ 3) measured by ⁷Li solid state NMR,” *Phys. Chem. Chem. Phys.*, vol. 9, no. 47, 2007, doi: 10.1039/b713311a.
- [7] L. Zhang *et al.*, “Enhancing the electrochemical performance of Li₄Ti₅O₁₂ anode materials by codoping with Na and Br,” *Journal of Alloys and Compounds*, vol. 903, 2022, doi: 10.1016/j.jallcom.2022.163962.
- [8] S. Loftager *et al.*, “A Density Functional Theory Study of the Ionic and Electronic Transport Mechanisms in LiFeBO₃ Battery Electrodes,” *The Journal of Physical Chemistry*, vol. 120, no. 33, 2016, doi: 10.1021/acs.jpcc.6b03456.
- [9] Berkeley Lab, “The Materials Project is powered by [open-source software](#), mp-685194: Li₄Ti₅O₁₂ (monoclinic, C2/c, 15),” <https://materialsproject.org/materials/mp-685194/>.
- [10] K. Kataoka *et al.*, “Single crystal growth and structure refinement of Li₄Ti₅O₁₂,” *J. Phys. Chem. Solids*, vol. 69, no. 5, pp. 1454-1456, 2007, doi: 10.1016/j.jpcs.2007.10.134.
- [11] K. Momma and F. Izumi, “VESTA 3 for three-dimensional visualization of crystal, volumetric and morphology data,” *J. Appl. Crystallogr.*, vol. 44, no. 6, 2011, doi: 10.1107/S0021889811038970.
- [12] P. Giannozzi *et al.*, “QUANTUM ESPRESSO: A modular and open-source software project for quantum simulations of materials,” *J. Phys. Condens. Matter*, vol. 21, no. 39, 2009, doi: 10.1088/0953-8984/21/39/395502.
- [13] M. Ernzerhof *et al.*, “Coupling-constant dependence of atomization energies,” *Int. J. Quantum Chemistry*, vol. 64, no. 3, pp. 285-295, 1997, doi: 10.1002/(SICI)1097-461X(1997)64:3<285::AID-QUA2>3.0.CO;2-S.
- [14] H. J. Monkhorst and J. D. Pack, “Special points for Brillouin-zone integrations,” *Phys. Rev. B*, vol. 13, no. 12, 1976, doi: 10.1103/PhysRevB.13.5188.
- [15] G. Henkelman, B. P. Uberuaga and H. Jónsson, “Climbing image nudged elastic band method for finding saddle points and minimum energy paths,” *J. Chem. Physics*, vol. 113, no. 22, 2000, doi: 10.1063/1.1329672.
- [16] Z. N. Ezhyeh *et al.*, “Review on doping strategy in Li₄Ti₅O₁₂ as an anode material for Lithium-ion batteries,” *Ceramics International*, 2022, doi: 10.1016/J.CERAMINT.2022.04.340.